Temporal electronic structure of non-resonant Raman excited virtual state of P-nitroaniline by 514 nm excitation via bond polarisabilities*

Wang Pei-Jie(王培杰)[a)†], Fang Yan(方 炎)[a)], and Wu Guo-Zhen(吴国祯)[b)]

[a)] *The Beijing Key Laboratory for Nano-Photonics and Nano-Structure, Capital Normal University, Beijing* 100048, *China*
[b)] *Molecular and Nano Sciences Laboratory, Department of Physics, Tsinghua University, Beijing* 100084, *China*

(Received 8 February 2010; revised manuscript received 12 March 2010)

We have studied the temporal bond polarisabilities of para-nitroaniline from the Raman intensities by the algorithm proposed by Wu *et al.* in 1987 (Tian B, Wu G, Liu G 1987 *J. Chem. Phys.* **87** 7300). The bond polarisabilities provide much information concerning the electronic structure of the non-resonant Raman excited virtual state. At the initial moment by the 514.5 nm excitation, the tendency of the excited electrons (mapped out by the bond polarisabilities) is to spread to the molecular periphery, and the electronic structure of the Raman virtual state is close to the pseudo-quinonoidic state. When the final stage of relaxation is approached, the bond polarisabilities of those peripheral bonds relax faster than those closer to the molecular core, the phenyl ring. The molecule is in the benzenoidic form as demonstrated by the bond polarisabilities after relaxation.

Keywords: Raman excited virtual state, bond polarisabilities, relaxation
PACC: 3220F, 7830C

1. Introduction

Raman scattering is a two-photon process involving vibronic coupling between excited electrons and nuclei. It is a powerful tool for studying molecular vibration. When a molecule is scattered by light, in general, it absorbs a photon first, accompanied with the excitation of its electrons, and then relaxes by emitting a second photon. In this process, the vibronic coupling can take place so that there is energy exchange between the electronic and the nuclear motions. The electronic excitation including its relaxation is called the Raman excited virtual state.[1] Here, only the non-resonance case is concerned, for the excited state is not an electronic eigenstate. For a typical Raman spectrum, there are two characteristics: one is the band position (frequency) and the other is its intensity (including the band shape). The former, determined by the strength of the chemical bonds, reflects the intra-molecular force field. The latter, determined by the bond polarisability derivatives, reflects the interaction between electrons and nuclei in the molecule. The vibronic coupling is parametrized by $\partial\alpha(t)/\partial Q_j$, which shows the response of the electronic charge to the nuclear motion. $\alpha(t)$ is called the electronic polarisability and Q_j the nuclear normal coordinate. For retrieving the electronic information about the virtual state, we should derive $\partial\alpha(t)/\partial S_k$ for the bond coordinates $S'_k s$. For brevity, $\partial\alpha(t)/\partial S_k$ is called the bond (stretch/bend) polarisability. It may reveal rich information about the temporal electronic structure of the non-resonant Raman excited virtual state.

The spectroscopic investigation of para-nitroaniline (PNA, 4-nitroaniline) has aroused special interest on account of its peculiar conjugation of single and double bonds with respect to the o- and m-nitroaniline.[2−7] PNA is a typical 'push-pull' molecule, which is characterized by an electron donating amino and an electron accepting nitro groups as shown in Fig. 1. Hence, it can be assumed to have different electronic configurations, benzenoidic (aromatic) or pseudo-quinonoidic, in different environments.[4] Two distinct electronic structures can be assumed for a push-pull molecule: one is a neutral form without formal charges on the donor and acceptor groups, and the other is a zwitterionic form. So PNA is an interesting system for studying vibrational dynamics as well as vibrational energy

*Project supported by the Natural Science Foundation of Beijing, China (Grant No. 2082006), the National Natural Science Foundation of China (Grant No. 20773073), the Key Grant Project of Chinese Ministry of Education (Grant No. 306020), and the Special Research Fund for the Doctoral Program of Higher Education, China (Grant No. 20060003050).
†Corresponding author. E-mail: Wangpeijie72@hotmail.com
© 2010 Chinese Physical Society and IOP Publishing Ltd

redistribution.[8]

In the present paper, we study the temporal bond polarisabilities of PNA from the Raman intensities. In the followings, the algorithm of elucidating bond polarisabilities is reviewed first. The experiment for recording the Raman intensities and a normal mode analysis are followed. Then, the elucidation and the interpretation of the bond polarisabilities are given. And finally, a concluding remark is presented.

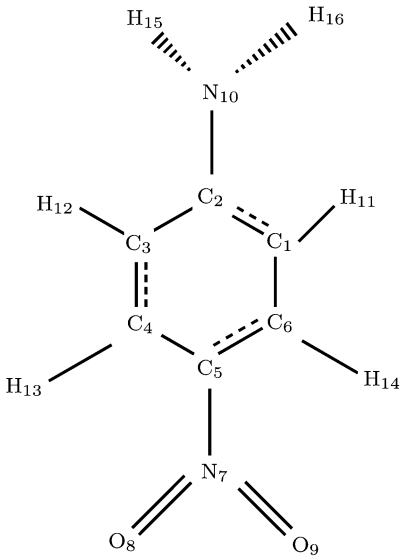


Fig. 1. Structure of p-nitroaniline (PNA) and its atomic numberings.

2. Algorithm

The algorithm for elucidating the bond polarisability from the Raman intensity was proposed by Wu group in 1987[9] and has been applied to several cases.[10−14] The main point is that the Raman intensity $I_j(t)$ of the j-th normal mode with frequency v_j is related to the electronic polarisability derivative with respect to its normal coordinate Q_j[15] via

$$I_j(t) \sim I_0 \frac{(v_0 - v_j)^4}{v_j} (\partial\alpha(t)/\partial Q_j)^2, \tag{1}$$

where I_0 is the intensity of the exciting laser with frequency v_0. One can transform the normal coordinate Q_j into the bond (internal) coordinates $S'_k s$ through the normal mode analysis by

$$S_k = \sum L_{kj} Q_j, \tag{2}$$

then Eq. (1) becomes

$$\pm\sqrt{I_j(t)} \sim \sqrt{I_0} \frac{(v_0 - v_j)^2}{\sqrt{v_j}} \sum L_{kj} (\partial\alpha(t)/\partial S_k). \tag{3}$$

By defining

$$a_{jk} = \frac{(v_0 - v_j)^2}{\sqrt{v_j}} L_{kj}, \tag{4}$$

we have the equation set in matrix notation as

$$\begin{pmatrix} P_1\sqrt{I_1(t)} \\ P_2\sqrt{I_2(t)} \\ \cdot \\ \cdot \\ \cdot \\ P_{3N-6}\sqrt{I_{3N-6}(t)} \end{pmatrix} = [a_{jk}] \cdot \begin{pmatrix} \partial\alpha(t)/\partial S_1 \\ \partial\alpha(t)/\partial S_2 \\ \cdot \\ \cdot \\ \cdot \\ \partial\alpha(t)/\partial S_{3N-6} \end{pmatrix}. \tag{5}$$

Here, the phase P_j is + or −, which cannot be obtained from the experiment or calculation, and needs determining. In this formalism, only the relative magnitudes of the Raman intensities are our concern. So are the relative bond polarisabilities. The relative bond polarisabilities can be figured out if the above equation set is inverted and if the phases can be determined.

3. Experiment

The Raman spectra were recorded by a microprobe Raman system (RENISHAW H 13325 spectrophotometer) with a CCD detector. A 50× objective was used to perform a backward scattering. The excitation line was 514.5 nm of Ar+ laser. The laser power on the sample was about 2.0 mW. The entrance-slit width was 50 μm and the integral time was 20 s.

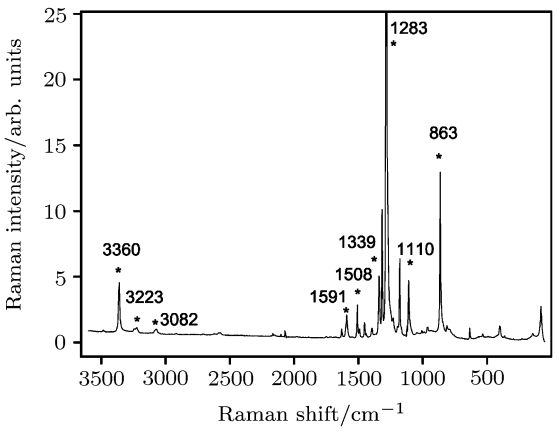


Fig. 2. Raman spectrum of solid p-nitroaniline by 514.5 nm excitation. Peaks marked with symbol ∗ refer to those modes whose intensities are employed for the elucidation of the bond stretching polarisabilities. Their Raman shifts and intensities are listed in Table 2.

The reagent of PNA of purity over 99% was used for the experiment. PNA is an organic compound with the formula $C_6H_6N_2O_2$ (consisting of a phenyl group attached to an amino group which is para to a nitro group) which is yellow solid crystal at room temperature. It was purchased from Aldrich Chemical Co. Ltd. For a careful intensity measurement, the polarisations of the Raman signals were taken into account. Their spectra were taken separately and then combined together for the corrections due to the different responses of the grating mirror and CCD detector in the various spectral ranges. For our purpose, only the relative intensities are considered. In the case where there is profile overlapping, and a deconvolution software is taken to resolve the profile into Lorentzian components. We estimate that the uncertainty of intensities is less than 20%. This will lead to about 10% uncertainty for the calculated bond polarisabilities. Figure 2 shows the Raman spectra of PNA by 514.5 nm excitation.

4. Normal mode analysis

The structural parameters and the force constants of PNA were obtained by density functional calculation. A normal mode analysis based on Wilson's GF matrix method[16] was used to obtain the $\boldsymbol{L}$ matrix through the fitting to the experimental mode frequencies. There are 42 ($3N$-6, $N = 16$) vibrational modes for PNA. The assignments were established by the analysis of the experimental spectra compared with those of o- and m-nitroaniline isomers.[17] The atomic numberings of PNA are shown in Fig. 1. The Local symmetry coordinates of PNA are defined and described in Table 1.

Table 1. Local symmetry coordinates of p-nitroaniline, where r and a denote the coordinates for the bond stretch and bond angle, respectively, τ denotes the coordinate for the out-of-CCC plane, and D denotes the dihedral angle.

definition	description
$S_1 = 2^{-1/2}[r(C1-C2)+r(C2-C3)]$	C–C symmetric stretching
$S_2 = 2^{-1/2}[r(C1-C2)-r(C2-C3)]$	C–C asymmetric stretching
$S_3 = 2^{-1/2}[r(C1-H11)+r(C3-H12)]$	C–H symmetric stretching
$S_4 = 2^{-1/2}[r(C1-H11)-r(C3-H12)]$	C–H asymmetric stretching
$S_5 = 2^{-1/2}[r(C1-C6)+r(C3-C4)]$	C–C symmetric stretching
$S_6 = 2^{-1/2}[r(C1-C6)-r(C3-C4)]$	C–C asymmetric stretching
$S_7 = 2^{-1/2}[r(C4-C5)+r(C5-C6)]$	C–C symmetric stretching
$S_8 = 2^{-1/2}[r(C4-C5)-r(C5-C6)]$	C–C asymmetric stretching
$S_9 = 2^{-1/2}[r(C4-H13)+r(C6-H14)]$	C–H symmetric stretching
$S_{10} = 2^{-1/2}[r(C4-H13)-r(C6-H14)]$	C–H asymmetric stretching
$S_{11} = r(C5-N7)$	C–N stretching
$S_{12} = 2^{-1/2}[r(N7-O8)+r(N7-O9)]$	N–O symmetric stretching
$S_{13} = 2^{-1/2}[r(N7-O8)-r(N7-O9)]$	N–O asymmetric stretching
$S_{14} = r(C2-N10)$	C–N stretching
$S_{15} = 2^{-1/2}[r(N10-H15)+r(N10-H16)]$	N–H symmetric stretching
$S_{16} = 2^{-1/2}[r(N10-H15)-r(N10-H16)]$	N–H asymmetric stretching
$S_{17} = 6^{-1/2}[2*a(H15-N10-H16)-a(H15-N10-C2)-a(H16-N10-C2)]$	N–H_2 scissoring
$S_{18} = 2^{-1/2}[a(H15-N10-C2)-a(H16-N10-C2)]$	N–H_2 rocking
$S_{19} = 2^{-1/2}[a(C1-C2-N10)-a(C3-C2-N10)]$	–N–H_2 in plane bending
$S_{20} = 2^{-1/2}[a(C2-C1-H11)-a(C6-C1-H11)]$	C–H in plane bending
$S_{21} = 2^{-1/2}[a(C1-C6-H14)-a(C5-C6-H14)]$	C–H in plane bending
$S_{22} = 2^{-1/2}[a(C4-C5-N7)-a(C6-C5-N7)]$	–N–O_2 in plane bending
$S_{23} = 2^{-1/2}[a(C3-C4-H13)-a(C5-C4-H13)]$	C–H in plane bending
$S_{24} = 2^{-1/2}[a(C2-C3-H12)-a(C4-C3-H12)]$	C–H in plane bending
$S_{25} = 6^{-1/2}[2*a(O8-N7-O9)-a(C5-N7-O9)-a(C5-N7-O8)]$	N–O_2 symmetric deformation
$S_{26} = 2^{-1/2}[a(C5-N7-O9)-a(C5-N7-O8)]$	–N–O_2 rocking
$S_{27} = 6^{-1/2}[a(C3-C2-C1)-a(C2-C1-C6)+a(C1-C6-C5)-a(C6-C5-C4)+a(C5-C4-C3)-a(C4-C3-C2)]$	ring trigonal deformation

Table 1. (*Continued*).

definition	description
$S_{28} = 12^{-1/2}[2 * a(C3 - C2 - C1) - a(C2 - C1 - C6) - a(C1 - C6 - C5)$ $+ 2 * a(C6 - C5 - C4) - a(C5 - C4 - C3) - a(C4 - C3 - C2)]$	ring asymmetric deformation
$S_{29} = 1/2[a(C2 - C1 - C6) - a(C1 - C6 - C5) + a(C5 - C4 - C3) - a(C4 - C3 - C2)]$	ring asymmetric deformation
$S_{30} = \tau(H11 - C1 - C2 - C6)$	C–H out of plane bending
$S_{31} = \tau(N10 - C2 - C3 - C1)$	$-NH_2$ out of plane bending
$S_{32} = \tau(H12 - C3 - C4 - C2)$	C–H out of plane bending
$S_{33} = \tau(H13 - C4 - C5 - C3)$	C–H out of plane bending
$S_{34} = \tau(N7 - C5 - C6 - C4)$	$-NO_2$ out of plane bending
$S_{35} = \tau(H14 - C6 - C1 - C5)$	C-H out of plane bending
$S_{36} = \tau(C5 - N7 - O8 - O9)$	$-NO_2$ out of plane bending
$S_{37} = \tau(C2 - N10 - H15 - H16)$	$-NH_2$ out of plane bending
$S_{38} = 6^{-1/2}[D(C1 - C2 - C3 - C4) - D(C2 - C3 - C4 - C5) + D(C3 - C4 - C5 - C6)$ $- D(C4 - C5 - C6 - C1) + D(C5 - C6 - C1 - C2) - D(C6 - C1 - C2 - C3)]$	ring puckering
$S_{39} = 1/2[D(C2 - C3 - C4 - C5) - D(C3 - C4 - C5 - C6)$ $+ D(C5 - C6 - C1 - C2) - D(C6 - C1 - C2 - C3)]$	ring asymmetric torsion
$S_{40} = 12^{-1/2}[-D(C1 - C2 - C3 - C4) + 2 * D(C2 - C3 - C4 - C5)$ $- D(C3 - C4 - C5 - C6) - D(C4 - C5 - C6 - C1)$ $+ 2 * D(C5 - C6 - C1 - C2) - D(C6 - C1 - C2 - C3)]$	ring asymmetric torsion
$S_{41} = D(O9 - N7 - C5 - C6)$	N–O torsion
$S_{42} = D(N15 - N10 - C2 - C3)$	N–H torsion

Mode symmetries can be classified by the point group C_{2V} even though the amino group (NH_2 group) is actually out of the molecular plane. From the normal mode analysis, we find that the coupling between bond stretching and bending coordinates is very small. This leads to the almost block-diagonalization of the L_{kj} matrix corresponding to the stretching and bending coordinate spaces. Hence, the phases that are mostly due to the bending motion, have little influence on the determination of the bond stretching polarisabilities.

For our purpose, we consider only the bond polarisabilities of the 9 bond stretches due to the molecular symmetry of C_{2V} (Hereafter, they, if without confusion, are simply called bond polarisabilities) Correspondingly, we need 9 mode intensities which are mostly composed of the bond stretching motions. They are marked by symbol $*$ in Fig. 2. Their Raman shifts and intensities and potential energy distributions are listed in Table 2. The mode intensity at 1283 cm^{-1} is normalized to 100 for convenience. The fitting errors of most frequencies are less than 1%.

Table 2. Experimental and fitted Raman shifts in cm^{-1}, relative intensities together with their potential energy distributions of p-nitroaniline.

experimental	fitted	intensity	potential energy distribution
3360	3355	9.5	$S15(100)$
3224	3223	1.4	$S9(99.8)$, $S5(0.2)$
3083	3082	0.4	$S3(99.8)$,$S1(0.2)$
1591	1600	5.1	$S5(45)$,$S1(21)$
1508	1509	4.3	$S7(26)$, $S1(13.7)$, $S14(4.3)$
1339	1343	6.2	$S12(77.6)$, $S11(28.5)$
1283	1276	100	$S14(54)$, $S5(10.7)$, $S1(4.9)$
1110	1111	4.3	$S11(30)$,$S7(28)$
863	858	18.9	$S7(15)$,$S1(13.7)$,$S12(10)$,$S11(8)$

5. Elucidation of bond polarisabilities

The Raman intensity $I_j(t)$ can be obtained from the experimental Raman signals in the wavenumber domain by Fourier transformation.[10] We note that in the normal Raman spectrum, the integrated Raman signal over wavenumber domain corresponds to the intensity in the time domain at $t = 0$ (the initial moment of the virtual state). This can be seen from the Fourier transform

$$\int I'_j(v)\mathrm{e}^{\mathrm{i}\,2\pi vt}\mathrm{d}v = I_j(t), \tag{6}$$

which, at $t = 0$, turns into

$$\int I'_j(v)\mathrm{d}v = I_j(0). \tag{7}$$

For the elucidation of the bond polarisabilities of the 9 stretching bonds, there are 2^9 possible phase combinations for the 9 mode intensities. Generally, the phase determination is a tough task. Fortunately, we have found that in most cases there is only one unique set or a limited number of phase sets that possess physical significance for the obtained bond polarisabilities. In the PNA case, we choose the phase set by considering that the elucidated bond polarisabilities of the C–C and C–H bonds are of the same signs (i.e., they are positive).[18] With this criterion, we are left with only 8 phase sets.

Among these 8 solution sets, there are three sets that lead the bond polarisability of C_3–H_{12} to be too much less than that of C_4–H_{13} (about 2 orders lower) or that of C_5–N_7 to be too much less than that of C_2–N_{10} (also about 2 orders lower). So, they are ruled out. For the remaining 5 solutions, we check their bond polarisabilities at the final stage of relaxation and require them to be congruent to the bond electron densities of the ground state[2,8] Thus another three phase sets are ruled out (The calculation of the bond electron densities of the ground state will be shown below.). Thereby only two phase sets remain. Among these two remaining candidate sets, one is with fluctuating bond polarisabilities as time evolves and it should be ruled out. Finally, we have only one phase set that leads to a reasonable physical consequence.

The elucidated bond polarisabilities at the initial and the final stages are shown in Fig. 3 in which the bond polarisabilities of C_1–C_6 are normalized to 10.

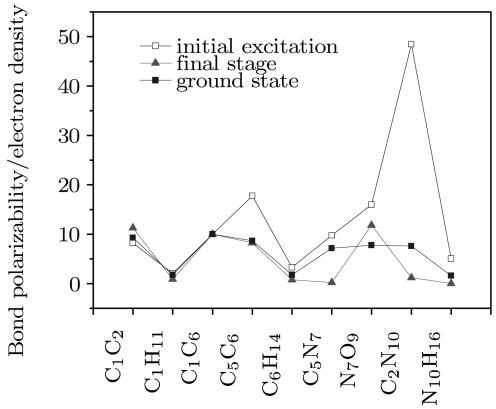


Fig. 3. Bond polarisabilities of p-nitroaniline at the initial excitation moment (□) and final stage (▲) of Raman relaxation. Symbol (■) is for the calculated bond electronic densities of the ground state. The values of C_1–C_6 bond are normalized to 10.

Shown in Fig. 4 are the bond polarisabilities each as a function of time, indicating the relaxation of the Raman excited virtual state. It is found that all the bond polarisabilities decay exponentially. The values of characteristic time t_c fitted by e^{t/t_c} are shown in Fig. 5.

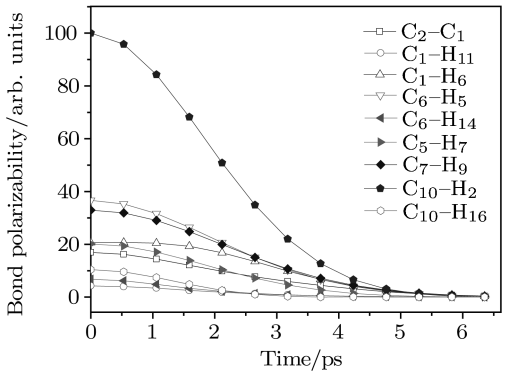


Fig. 4. Curves for bond polarisabilities of p-nitroaniline by 514.5 nm excitations as a function of time. The value for C_2–N_{10} bond at $t = 0$ is normalized to 100.

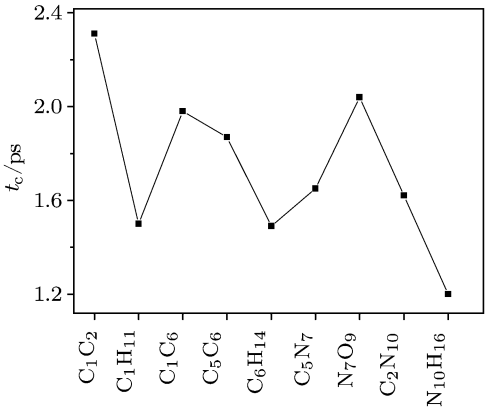


Fig. 5. Characteristic times for the relaxations of the various temporal bond polarisabilities of p-nitroaniline by 514.5 nm excitation.

The values of bond electron density ρ_t of the ground state are calculated by RHF/6-31G*, with the polarisabilities of the C_1–C_6 bond normalized to 10. They are plotted in Fig. 3. ρ_t is computed from

$$\rho_t = \sum_{\gamma}\sum_{ij} C^{\alpha}_{i\gamma} C^{\beta}_{j\gamma} S^{\alpha\beta}_{ij}, \tag{8}$$

where i and j are the labelings, respectively, for the atomic orbitals of atoms α and β which form bond t; γ is the labeling for the occupied molecular orbitals; C and S are the linear combination coefficient and overlap integral, respectively. We need bond electron densities in elucidating bond polarisabilities in the later analysis.

6. Results and discussion

At the initial excitation moment, the bond polarisabilities of the C_2–N_{10}, C_5–C_6 (C_4–C_5) (and probably, N_7–O_9 (N_7–O_8)) bonds are larger than their values at the final stage of relaxation (around 6 ps). At the final stage of relaxation, the bond polarisabilities of the C–C bonds of the molecular ring are quite the same, indicating the benzenoidic form. This demonstrates that the tendency of the excited electrons is to spread to the molecular outer portion, the C_2–N_{10} bond, from the phenyl ring. Similar situation also appears in the 2-aminopyridinde case where the C–N bond connected with the aromatic ring possesses the largest bond polarisability in the initial stage of the Raman virtual state.[12] Therefore, electronic structure of the virtual state is close to the pseudo-quinonoidic form rather than the benzenoidic form after relaxation (or the ground state).

As shown in Fig. 5, the bond polarisability of N_{10}–H_{16} (N_{10}–H_{15}) decays much faster than those of the remaining bonds. The decay rates of the bond polarisabilities of C_1–H_{11} (C_3–H_{12}) and C_6–H_{14} (C_4–H_{13}) which are in the molecular periphery are similar and smaller than that of N_{10}–H_{16} (N_{10}–H_{15}). The bond polarisabilities of C_5–N_7 and C_2–N_{10}, which are the bridges between the nitro and amino groups and the phenyl ring, are with even slower decay rates. The relaxations of the bond polarisabilities of C_1–C_2 (C_2–C_3), C_1–C_6 (C_3–C_4), and C_5–C_6 (C_4–C_5) of the phenyl ring are the least in all relaxations of the bond polarisabilities. These observations confirm again that the excited electrons at the initial stage tend to flow to the peripheral bonds, so that during relaxation, the polarisabilities of these bonds will relax faster as the electrons flow back to the phenyl ring. Finally, we note that the bond polarisability of N_7–O_8 (N_7–O_9) does not relax so fast as a peripheral bond. This may be due to the electron localization on the NO_2 group in the Raman process.

7. Conclusion

The temporal electronic structure of the non-resonant Raman excited virtual state of PNA by 514 nm excitation is studied by the bond polarisabilities. At the initial excitation moment, the tendency of the excited electrons (mapped out by the bond polarisabilities) is to spread to the molecular periphery and the electronic structure of Raman virtual excited state is close to the pseudo-quinonoidic state. When the final stage of relaxation is approached, the relative magnitudes of the bond polarisabilities are congruent to the bond electron densities of the ground state correspondingly. This corresponds to the benzenoidic form. Furthermore, we suppose the electron localization on NO_2 group in the Raman process from the characteristic decaying time of its bond polarisability.

This algorithm has potential applications in exploring the other Raman fields such as surface-enhanced Raman scattering (SERS) provided that their nice Raman profiles can be obtained.

References

[1] Fang C and Wu G 2007 *J. Raman Spectrosc.* **38** 1416
[2] Harrand M 1975 *J. Raman Spectrosc.* **4** 53
[3] Epstein L M, Shubina E S, Ashkinadze L D and Kasitsyna L A 1982 *Spectrochim. Acta* Part A **38** 317
[4] Marlow F, Hill W, Caro J and Finger G 1993 *J. Raman Spectrosc.* **24** 603
[5] Maurizio M M 1997 *J. Raman Spectrosc.* **28** 205
[6] Kozich V, Werncke W, Dreyer J, Brzezinka K W, Rini M, Kummrow A and Elsaesser T J 2002 *Chem. Phys.* **117** 719
[7] Fraztdinov V M, Chanz R, Kovalenko S A and Ernsting N P 2000 *J. Phys. Chem.* A **104** 11486
[8] Kozich V, Werncke W and Dreyer J 2002 *J. Chem. Phys.* **17** 719
[9] Tian B, Wu G and Liu G 1987 *J. Chem. Phys.* **87** 7300
[10] Fang C, Liu Z and Wu G 2008 *J. Mol. Struct.* **885** 168
[11] Liu Z and Wu G 2005 *Chem. Phys.* **316** 25
[12] Wang H and Wu G 2006 *Chem. Phys. Lett.* **421** 460
[13] Liu Z J and Wu G Z 2006 *Acta Phys. Sin.* **55** 6315 (in Chinese)
[14] Fang C and Wu G 2009 *Acta Phys. Sin.* **58** 2345 (in Chinese)
[15] Chantry G W 1971 *Polarisability Theory of the Raman Effect*, in: Anderson A (Ed.) The Raman Effect, vo1. 1, (New York: Marcel Dekker Inc.) p1
[16] Wilson Jr E B, Decius J C and Cross P C 1955 *Molecular Vibrations* (New York: McGraw-Hill) p11
[17] Tanaka T, Nakajima A, Watanabe A, Ohno T and Ozaki Y 2003 *J. Mol. Struct.* **661** 437
[18] Yoshino T and Bernstein H J 1959 *Spectrochim. Acta* **14** 127